Available online at www.sciencedirect.com
SCIENCE DIRECT®
ELSEVIER
Journal of Nuclear Materials 322 (2003) 111–118
journal of nuclear materials
www.elsevier.com/locate/jnucmat

Cerium oxidation during leaching of CeYSiAlO glass

S. Gavarini [a,b,*,1], M.J. Guittet [c], P. Trocellier [d], M. Gautier-Soyer [c], F. Carrot [a], G. Matzen [b]

[a] Laboratoire Pierre Süe, CEA-CNRS, UMR 9956, CE Saclay, 91191 Gif sur Yvette, France
[b] CRMHT, CNRS UPR 4212, 1D Avenue de la Recherche Scientifique, 45071 Orléans cedex 2, France
[c] SPCSI, CEA/DSM/DRECAM, CE Saclay, 91191 Gif sur Yvette, France
[d] SRMP, CEA-DEN/DMN, CE Saclay, 91191 Gif Sur Yvette, France

Received 6 January 2003; accepted 20 June 2003

Abstract

The chemical stability of a CeYSiAlO glass was examined after leaching with bidistilled water (autoclave: $T = 90$ °C) during 1 month. The initial S/V ratio was approximately 0.06 cm^{-1} and the pH was free to drift during the experiments (initial pH $\approx$ 5.5). The leached samples were analyzed using scanning electron microscopy coupled with energy disperse X-ray spectrometer, X-ray photoelectron spectrometry and X-ray diffraction. Dissolution kinetics were also followed by inductively coupled plasma mass spectrometry and spectrophotometry analyses of the liquid medium. The results indicate that Ce is oxidized during leaching which results in the formation of a thick amorphous Ce(IV)-containing layer, possibly CeO_2 with Y and probably −OH (and/or H_2O) species. It is hypothesized that the low solubility of Ce(IV) oxide (and/or hydroxide) is mainly responsible for the formation of this layer, thus, preventing the release of Y and Ce and to a lesser extent of Si and Al after a few days of leaching.

PACS: 61-10.N; 79-60; 68-37.H; 82-80; 82-60.H; 68-35.D; 82-60.L; 82-20; 82-40; 61-20

1. Introduction

Rare earth quaternary aluminosilicate glasses are potential matrices for the long-term storage of trivalent actinides produced by the nuclear industry [1,2]. They present exceptional mechanical and chemical properties [1–6], particularly when Y is added in the glass composition [1,2,5,7–10]. Rare earth elements (REE) have chemical properties close to the trivalent transuranium elements [11–20]. The REE content (5 at.% in glass studied here) in the glasses contributes to the disorder of the network [5,6,21] due to the important field strength of such trivalent cations ($\sim q/r^2$; q: charge and r: ionic size). This last property results also in a high fusion temperature (T_f) and glass transition temperature (T_g) for this family of glasses, approximately 1600 and 880 °C, respectively [1,2,6–8,22–25]. The formation of AlO_4^- tetrahedra stabilizes the excess positive charge of Y^{3+} and REE^{3+} [4,8]. NMR experiments have demonstrated on analogous glasses, containing lanthanum, that Al_V and Al_{VI} (Al in fivefold and sixfold coordination, respectively) fractions increase with La/Si ratio, but fourfold Al remains dominant [1,2,21]. Shelby et al. [8] have suggested Al_V and Al_{VI} would decrease the clustering which is necessary for the local charge balance of Y^{3+} (and thus REE^{3+}) in these networks, thus, reducing the formation of segregated regions in the melt. At least, Sen [26] showed, using EXAFS on NdSiAlO glasses, that Nd ions are predominantly surrounded by Al units. The aim of the present study is to examine the influence of Ce, which has two stable oxidation states (III or IV), on the

* Corresponding author. Tel.: +33-472 44 83 59; fax: +33-472 44 80 04.
E-mail address: s.gavarini@ipnl.in2p3.fr (S. Gavarini).
[1] On leave from UMR 5822, Institut de Physique Nucléaire de Lyon, Bât. Paul Dirac, 4 rue Enrico Fermi, 69622 Villeurbanne cedex, France.

0022-3115/$ - see front matter
doi:10.1016/S0022-3115(03)00306-4

dissolution mechanisms of CeYSiAlO glasses. In pristine CeYSiAlO glasses, the main oxidation state of Ce is Ce(III) [25]. However, the coexistence of Ce(III) and Ce(IV) may influence glass formation and structure. The knowledge on multivalent elements behavior during leaching is, therefore, pertinent for actinide confinement in glass matrices.

2. Experimental protocols

2.1. Glass synthesis

The synthesis process has been extensively described elsewhere [27,28]. Briefly, oxide melts were prepared with the following oxides: Al_2O_3, SiO_2, Y_2O_3 and CeO_2. Glasses were synthesized at ambient atmospheric concentrations in a 220 V Joule effect furnace equipped with a Pt crucible. The annealing process was subsequently performed in a furnace at 880 °C over 5 h. The glasses were then cooled to room temperature during a period of 15 h (1 °C/min). Scanning electron microscopy coupled with energy disperse X-ray spectrometer (SEM–EDS) analyses on several of the glasses indicated that the experimental composition was similar to that predicted theoretically (Table 1) with no detected impurity being greater than 0.5 at.%. On completion of the synthesis process, X-ray diffraction (XRD) analyses, using Cu electrode X-ray emission (CuKα), has confirmed that no crystalline phase was present in the glassy matrix (Fig. 5). Before the leaching experiments, monoliths of glass were cut with a diamond wheel and polished to 0.3 μm using SiC disks and Al_2O_3 powder.

2.2. Leaching tests

Leaching tests were performed in 50 ml Teflon™ containers. The volume of leachate used was equivalent to a S/V ratio equal to 0.06 cm^{-1} (S: geometric surface of the monolith in cm^2; V: volume of the leachant in cm^3). Glass monoliths were placed on a Teflon basket, before submersion in the liquid, to maximize the surface of the glass in contact with solution. Bidistilled water (Micropore™ system) was used as the leachate (pH 5.5). Teflon containers were placed in an autoclave at 90 °C and leaching was conducted over 33 days with samples being taken after 0.6, 4, 7, 16, 21, 28 days. At each sampling time the container was opened after decreasing the temperature of the oven to ambient conditions, and an aliquot of solution (between 100 and 300 μl) was sampled. The modification of the S/V ratio, after 33 days, was lower than 5% with a final S/V ratio of approximately 0.065 cm^{-1}. A blank was also prepared to ensure that pH and solution elemental concentrations were due to glass dissolution.

2.3. Solution analysis

One aliquot of the solution samples was acidified while the remainder was ultra-filtered (membrane with 1.8 nm pore size under 4 bar N_2 pressure) to determine the quantity of colloidal/particles compounds. Solution analysis of Y, Ce and Al was performed by inductively coupled plasma mass spectrometry (ICP-MS). Si was quantified by spectrophotometry analysis using the molybdate blue method. The detection limits of these two techniques are, respectively, 0.02 ppb and 0.2 ppm. The normalized releases (superficial mass loss in $\mu g/m^2$) were calculated according to the relation:

$$\mathrm{NL}_i = \frac{C_i V}{S f_i} \ (\mu g/cm^2), \tag{1}$$

where 'C_i' is the mass concentration of the element 'i', 'V' the volume of leachate in cm^3, 'S' the geometric area of the sample in cm^2 and 'f_i' the mass fraction of the element 'i' in the glass.

2.4. Solid analyses

The glass monoliths were prepared for analyses, after leaching, by washing with bidistilled water and then drying at 105 °C in a regulated autoclave for 2 h. A graphite coating layer of approximately 20 nm was then applied on a part of the glass in order to obtain good surface conductivity. Solid analyses were performed using a SEM–EDS. The electron beam energy can vary between 15 and 30 keV and the volume probed under these conditions is approximately 1 μm^3. XRD (CuKα radiation, Philips PW1729 diffractometer, Eindhoven, The Netherlands) at room temperature was used to identify the crystalline phases. The XRD acquisition parameters were: $10° < 2\theta < 70°$, step = 0.02°, 20 s/deg.

X-ray photoelectron spectrometry (XPS) experiments were performed with a non-monochromated $Al_{K\alpha}$ source

Table 1
Nominal and experimental (SEM–EDS analysis) composition of CeYSiAlO pristine glass

Glass[a]	Si (at.%)	Al (at.%)	Y (at.%)	Ce (at.%)	O (at.%)	Al/Si	Y/Ce	(Al+Si)/(Y+Ce)
CeY nom.	14.1	12.8	5.1	5.1	62.8	0.91	1.00	2.64
CeY exp.	14.7	13.1	5.5	5.5	61.0	0.89	1.00	2.53

[a] Nom. = nominal calculated composition for oxide melt, exp. = experimental composition of the glass.

at a base pressure of 5×10^{-10} mbar using a VG Escalab Mark II™. The analysis chamber included an aluminium anode. The hemispherical analyser was fitted with five-channeltron detection and operated with a 20 eV pass energy. As the samples were insulating, energy calibration was achieved by setting the binding energy of carbon at 284.6 eV.

3. Results

3.1. Solution analyses

3.1.1. Evolution of pH

The results of the pH-measurements during leaching are displayed in Fig. 1. The curve for the CeY glass indicates a strong decrease of H^+ concentration in solution with a corresponding increase of pH from 5.5 to 10–11 during the first stage of the experiment, pH then slightly decrease (probably because of the equilibrium with atmospheric carbon dioxide), to finally remain stable near a value of 10 until the end of the leaching process. In comparison, the pH of the blank solution stayed between pH 5 and 7 throughout the experiment.

3.1.2. Elemental release

The normalized loss values (noted NL as indicated in Eq. (1)), for Si, Al, Y and Ln (La or Ce), after each time period, are presented in Fig. 2. Greatest dissolution occurred for Si followed by Al, whereas NL_Y and NL_{Ce} dissolution was much lower. The final pH value of 10 corresponds to the minimum solubility of Y/REE tri-hydroxide compounds according to the literature: $\log[Y(III)_{sol.}] = -9.5$ and $\log[Ce(III)_{sol.}] = -8.5$, at pH = 9 and $T = 298$ K [29]. The experimental elemental concentrations in mol/l are compared to theoretical solubility of reference products at 25 °C and pH 10 in Table 2 (reference products: vitreous silica, gibbsite, Y or Ce(III) tri-hydroxide and cerium(IV) dioxide). Si release is relatively far from solubility limit ($SiO_{2\,vitreous} + 2H_2O \leftrightarrow H_4SiO_4 \leftrightarrow H_3SiO_4^- + H^+ \leftrightarrow H_2SiO_4^{2-} + 2H^+$ (4), $\log K_1 = -2.8$, $\log K_2 = -9.17$, $\log K_3 = -10.17$ [30–32]), whereas Al, Y and Ce are over saturated ($Al(OH)_3 + 3H^+ \leftrightarrow Al^{3+} + 3H_2O$ (3), $\log K = 8.5$ [29]). This last observation is explained by the presence of colloids or particles as shown by ultra-filtration. These colloids represent 97%, 90%, 82% and 12% of the total amount of Ce, Y, Al and Si in solution respectively (the normalized loss displayed in Fig. 2 include colloids and/or particles).

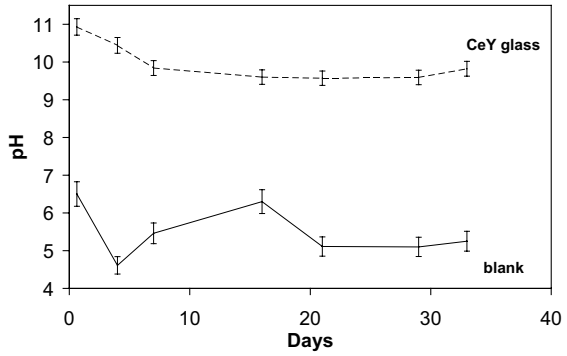

Fig. 1. Evolution of pH during leaching of CeYSiAlO glass ($pH_i = 5.5$).

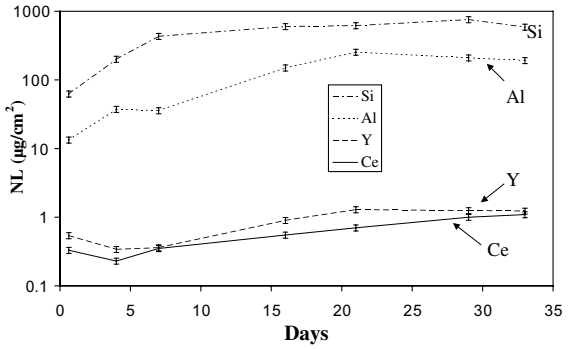

Fig. 2. Cumulative normalized losses (NL, in g/cm^2) during leaching.

3.2. Solid analyses

3.2.1. Secondary electron imaging

The surface of altered glass was observed using secondary electrons and the resulting pictures are displayed in Fig. 3. These analyses revealed a cracked and glossy

Table 2
Experimental release values in solution after 33 days of leaching and solubility limit in mol/l for each element of the glass (reference products involved in solubility calculations: vitreous silica, gibbsite, Y/Ce(III) tri-hydroxide and Ce(IV) dioxide [20–23])

	Si (mol/l)	Al (mol/l)	Y (mol/l)	Ce (mol/l)
Experimental release	1.7^{-4}	5.0^{-5}	1.3^{-7}	1.2^{-7}
Solubility limit	1.9^{-2}	1.0^{-4}	3.2^{-10}	Ce(III) 8.0^{-8} Ce(IV) 7.0^{-49}

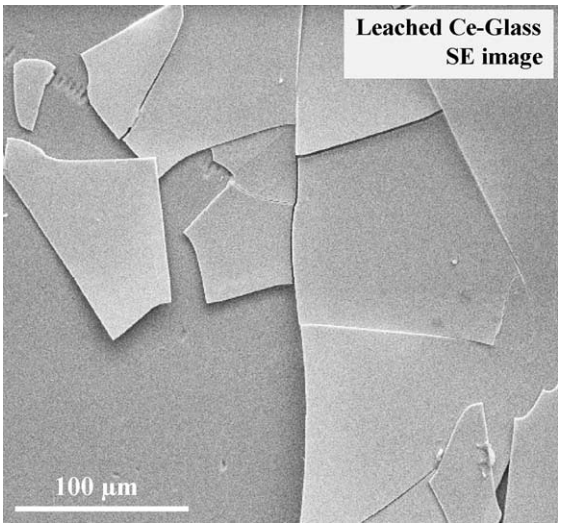

Fig. 3. Secondary electron image of the glass surface after 33 days of leaching.

layer of about 2–3 μm thickness that had become detached from the glass surface in some places. Cracks are probably a consequence of drying and/or submitting samples to vacuum conditions. One can suppose that the alteration layer just after leaching was covering homogeneously the whole surface of the glass.

3.2.2. SEM–EDS analyses

The results of SEM–EDS analyses on pristine glass and the alteration layer are summarized in Table 3 (see also Table 1). After leaching, there is a strong (Y,Ce)-enrichment at the glass surface which correlates with an (Al,Si)-depletion. The penetration depth of the electron beam in these materials is approximately 1 μm. As a consequence, variations of composition occurring deeper than 1 μm cannot be characterized by this technique. Therefore the percentages presented here are not directly comparable with total solution release values displayed in Fig. 2. To estimate more precisely the thickness of altered layer and to visualize potentially deeper compositional variations, X-ray emission mapping was also performed on transversal sections of the altered glass (Fig. 4). This analysis confirmed the results displayed in Table 3 with an important (Y,Ce)-enrichment in the altered region correlating with (Al,Si)-depletion. The thickness of the altered layer was evaluated on the secondary electron image to 4–5 μm. The spatial resolution was limited by the volume probed in subsurface by this technique (typically 1 μm^3), which precludes the characterization of slight compositional gradients. However, a clear composition frontier is observed between altered region and what appears to be the almost unaltered glass beneath.

Table 3
SEM–EDS elementary quantification for the pristine and altered glass (at.%)

X-ray detection	$O_{K\alpha}$	$Al_{K\alpha}$	$Si_{K\alpha}$	$Y_{L\alpha}$	$Ce_{L\alpha}$
Pristine glass	61.0	13.1	14.7	5.5	5.5
Altered glass	67.1	4.2	10.0	9.6	8.9

3.2.3. XRD analyses

The diffraction pattern of the pristine and altered glasses, as well as a crystalline CeO_2 reference spectra, are displayed in Fig. 5. No crystalline phase was observed for both of the glasses, with a typical vitreous signal located between $\theta = 10°$ and 40°. A comparison with the crystalline CeO_2 spectra revealed a broad band present at the position of the first crystalline CeO_2 peak

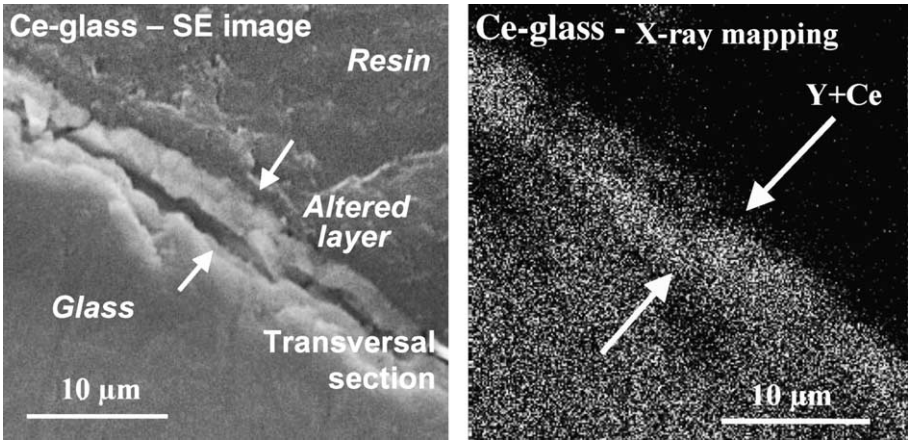

Fig. 4. Secondary electron image and X-ray elementary mapping (Y + Ce) of a transversal section of the glass altered during 33 days.

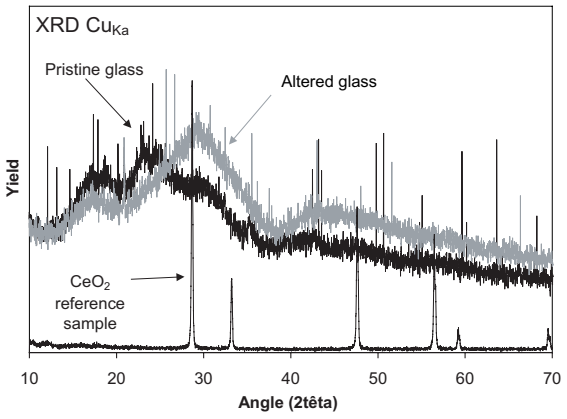

Fig. 5. Diffraction pattern for pristine glass (black line), altered glass (grey line) and crystalline CeO_2 (black line with peaks).

for the altered glass. This suggests that the alteration layer formed at the glass/solution interface during leaching is highly amorphous CeO_2.

3.2.4. XPS analyses

The XPS analysis was used to determine the oxidation state of cerium near the surface before and after leaching. Both Ce(III) and Ce(IV) show the $3d_{5/2}$ and $3d_{3/2}$ multiplet, but for the latter, each component ($3d_{5/2}$ and $3d_{3/2}$) shows three peaks instead of two [33,34]. In the case of Ce(IV), a peak is also observed at a binding energy of 916 eV. This corresponds to the initial state of tetravalent cerium (called 'f^0' configuration) that is not found in the initial state of trivalent cerium [35–37], and was useful to identify the IV-valence of cerium at the glass surface after leaching. This peak (called P6 in the following) is not observed for Ce(III) and it is thus possible to differentiate the two oxidation states. A CeO_2 reference was used to obtain a spectrum corresponding to Ce(IV), and the characteristic signal of Ce(III) was obtained with pristine glass that mainly contains the III-valence. XPS spectra for pristine glass, altered glass and the CeO_2 reference sample are represented in Fig. 6. To simplify the notation, for each multiplet corresponding to a different spin/orbital coupling ($J = 3/2$ or 5/2), the peaks are called 'P_i', with i: a number for Ce(IV) peaks and a letter for Ce(III) peaks. The Ce 3d lines of pristine glass are characteristic of mainly Ce(III), even if a small amount of Ce(IV) may be observed as indicated by the weak signal at 916–917 eV in Fig. 6(b). Fig. 6(c) shows that the altered glass surface contains a mixture of Ce(IV) and Ce(III).

Spectra were also acquired for energy regions corresponding to Si_{2s} and Y_{3d} lines as shown in Fig. 7 for pristine and altered glass. The satellite peak is due to excitation of Y_{3d} by the $Al_{K\alpha}$ line (non-monochromatized X-ray source). The Si_{2s} peak is weaker relatively to

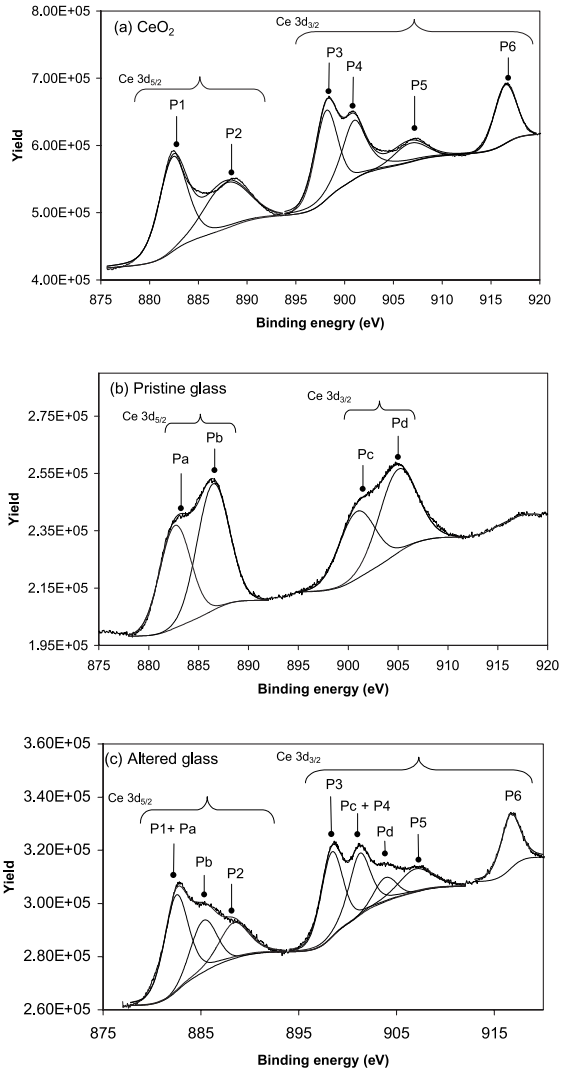

Fig. 6. X-ray photoelectron spectrometry spectra (Ce $3d_{5/2}$ and Ce $3d_{3/2}$ lines) for crystalline CeO_2, pristine and altered glass.

the Y_{3d} peak for the altered glass (Fig. 7(b)) when compared with the pristine sample (Fig. 7(a)). This confirms the Y/Si relative enrichment of the surface layer after leaching as demonstrated by SEM–EDS analysis. The resulting deconvolution of these curves (Figs. 6 and 7) are summarized in Table 4 for (un-)altered glass and CeO_2. A notable shift is observed between the pristine and leached glasses concerning the binding energy of the peak Pd (905.3 and 904.0 eV respectively). This could be due to the high density of the peak observed for the altered glass, leading to a less precise deconvolution. However, they remain close enough to CeO_2 and the pristine glass peak positions to attribute them to Ce(IV) and Ce(III).

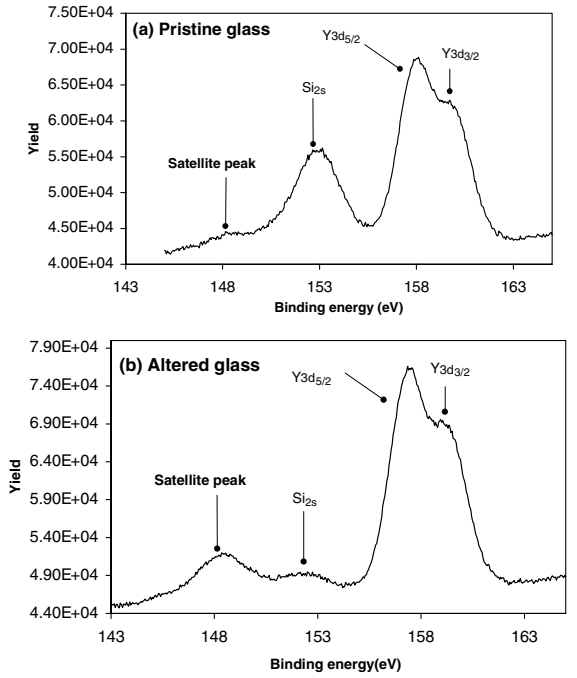

Fig. 7. X-ray photoelectron spectrometry spectra ($Si_{2s} + Y_{3d}$ lines) for pristine and altered glass.

4. Discussion

The oxidation of Ce(III) into Ce(IV) occurring during leaching of CeYSiAlO glass leads to the formation of a Ce-enriched superficial layer. However, the quantity of Ce(III) remaining in the glass surface after this treatment indicates that cerium oxidation is not complete. The positions of XPS peaks corresponding to oxidized cerium in leached sample are very close to those of crystalline CeO_2, but it is however difficult to determine if the formed phase is an oxide, an hydroxide or a mixing of both. Its highly disordered nature has been demonstrated by XRD analyses. The diffraction pattern exhibits a broad signal with maximum located close to the emplacement of crystalline CeO_2 peak suggesting the possible formation of amorphous cerium dioxide. SEM–EDS analysis also showed an important Y-enrichment at the surface together with a strong (Si,Al)-depletion. Yttrium is more retained than Si and Al in the alteration layer probably because of its very low solubility as $Y(OH)_3$ near pH 10. However, if we consider that the cumulative normalized loss of Si and Al reaches a plateau after 15–20 days of leaching, this accounts for protective properties of the superficial barrier increasing with time. The reaction probably involved in cerium oxidation is: $Ce(III) + H^+ + \frac{1}{4}O_{2(g)} = Ce(IV) + \frac{1}{2}H_2O$ (2) [29]. This probably contributes to the increased pH during leaching but it is not sufficient to account for the final value around 10–11. At this pH value, OH^- ions must be compensated by cations in a similar concentration range. As cations coming from the leaching of the glass can be mainly $Y(OH)_n^{(3-n)+}$ and $Ce(OH)_n^{(3-n)+}$ at this pH, cations are apparently lacking (excess of negative charges about 2.5×10^{-4} mol/l, mainly silicate species $H_3SiO_4^-$ and $H_2SiO_4^{2-}$). Si and Al are mainly under anionic forms (anionic silicate species and $Al(OH)_4^-$) and the presence of cations including Ce(IV) is limited by its low solubility. This high pH may be due to the release of alkaline or alkaline-earth elements such as Na^+ likely to be present as a minor component in the pristine glass. This increased pH probably plays a role in the strong accumulation of Ce at the surface of the glass as the solubility of this element decreases with increasing pH. However, cerium oxidation has been also observed (using XPS) after dynamic leaching experiments carried out in Soxhlet device (see [38] for preliminary results), where the leachate is renewed ($T \approx 100$ °C) and presents a relatively stable pH between 5 and 7 because of the permanent equilibrium with atmosphere. The main consequence of the increased pH in static conditions could thus be an enhancement of Ce(IV) re-deposition on the surface of the glass. This process is also favoured by a probable M^+/H^+ interdiffusion process (with M^+ = alkaline or alkaline earth from the glass, and

Table 4
Results of the decomposition of XPS spectra: $Ce3d_{5/2}$, $Ce3d_{3/2}$, Si2s and Y2p

Samples	Charge (eV)	Si 2s (eV)	Y 3d (eV)	Ce $3d_{5/2}$ (eV)	Ce $3d_{3/2}$ (eV)
Leached glass	5.0	151.8	159.4	P1 Ce^{4+}/Pa Ce^{3+}: 882.8	P4Ce^{4+}/Pc Ce^{3+}: 901.3
			157.3	P2 Ce^{4+}: 888.6	P5 Ce^{4+}: 907.2
				P3 Ce^{4+}: 898.4	P6 Ce^{4+}: 916.7
				Pb Ce^{3+}: 886.0	Pd Ce^{3+}: 904.0
Pristine glass	13.1	153.5	160.7	Pa Ce^{3+}: 882.7	Pc Ce^{3+}: 901.4
			158.6	Pb Ce^{3+}: 886.4	Pd Ce^{3+}: 905.3
CeO_2	11.3			P1 Ce^{4+}: 882.5	P4 Ce^{4+}: 901.0
				P2 Ce^{4+}: 888.3	P5 Ce^{4+}: 906.9
				P3 Ce^{4+}: 898.1	P6 Ce^{4+}: 916.4

H^+ = protons from the solution), as it is extensively described for alkaline borosilicate glasses [39–44]. This interdiffusion involving minor components of the glass could occur on several micrometers, thus enhancing water incorporation in the material and chemical bonds hydrolysis. Experiments in static conditions with a stronger control of the pH would be necessary to ensure that an equally thick superficial layer is formed for a pH fixed around 5.5. If we compare releases in solution of CeYSiAlO glass with those of simplified alkaline borosilicate glass (composition in at.%; Nd: 0.5, Si: 16.7, Al: 2.3, B: 9.0, Na: 7.0, Ca: 1.8, Li: 2.6, Fe: 0.7, Mo: 0.4) leached in the same conditions [27,28], it appears that Si release is slightly lower here ($NL_{Si} = 1000 \pm 50$ μg/cm^2 for SON 68 glass and 600 ± 30 μg/cm^2 for CeYSiAlO glass). However, Si does not provide an ideal indication about the dissolution of the glass because it could be involved in re-precipitation of secondary phases (contrarily to Na for instance). REE release is slightly higher for CeYSiAlO glass but remains comparable with that of SON 68 glass ($NL_{REE} = 0.4 \pm 0.02$ μg/cm^2 for SON 68 glass and 1.2 ± 0.06 μg/cm^2 for CeYSiAlO glass). More than 90% of REE and Y found in solution are present as colloid or particles due to their very low solubility at pH 10 (and about 80% for Al). The globally low solubility of Ce(IV)-compounds in basic conditions represents a guarantee for the chemical protection of CeYSiAlO glass. This property is very interesting in the perspective of a storage in clay geological media for instance where groundwater is almost static and slightly alkaline.

5. Conclusion

A change in the oxidation state of Ce has been demonstrated for CeYSiAlO glass leached in static conditions at 90 °C in initially bidistilled water. An amorphous (Ce,Y)-enriched layer is formed at the surface probably favoured by the very low solubility of Ce(IV) compounds such as CeO_2 (or hydroxide). A superficial (Si,Al)-depletion was outlined, however, Si and Al normalized losses reach a plateau after 15–20 days of leaching indicating a protective role of the alteration layer increasing with time. The strong increase of pH is not well understood and could be a consequence of the interdiffusion process between protons of the solution and alkaline (and/or alkaline earth) cations likely to be present in the pristine glass as minor components. As a conclusion, CeYSiAlO glass presents a good chemical durability, mainly because of the retention properties of the Ce-rich superficial layer formed in basic conditions. Normalized loss values are close to those measured for French SON68 glass leached in the same conditions initially. However, SON68 glass is characterized by the high flexibility of its structure that can incorporate a great variety of elements such as actinides and fission products. In comparison, glasses studied here do not contain any alkaline element as major component and the resulting less flexible structure would thus be more adapted to the specific immobilization of trivalent or tetravalent actinides (in substitution of a part of the REE). As a matter of fact, the retention properties of CeYSiAlO glass concerning mobile radioelements such as Cs or I are not known (contrarily to French SON68). Moreover, other effects have to be taken into account for long term predictions, such as alpha-induced surface radiolysis, particularly in the case where actinides are accumulated together with REE near the surface. Note also that, in the present case, the oxidation of Ce leads to the formation of an insoluble compound that plays a protective role, but cases exist were the oxidized state of rare earth or actinide is much more soluble than the reduced form (as for uranium: U(VI) more soluble than U(IV)), possibly resulting in an overall increase of the rate of dissolution, as showed for UO_2 [45]. For these reasons, parameters such as composition, pH (generally basic) and redox potential (generally reducing) of natural groundwater have to be well known in the perspective of a storage of nuclear waste in geological repository.

Acknowledgements

We thank A. Douy and E. Veron (CRMHT, Orléans CNRS) for their precious advice and expertise in XRD experiments. Thanks are also due to Y. Vaills (CRMHT, Orléans CNRS) for his help during glass synthesis. Special praise goes to Richard Collins for improving the English of this article.

References

[1] L. Bois, M.J. Guittet, N. Barré, P. Trocellier, S. Guillopé, M. Gautier, P. Verdier, Y. Laurent, J. Non Cryst. Solids 276 (2000) 181.
[2] S. Guillopé, thesis, University of Rennes 1, France, 1999.
[3] A. Aronne, Mat. Chem. Phys. 51 (1997) 163.
[4] J.T. Kohli, R.A. Condrate, Phys. Chem. Glasses 34 (3) (1993) 81.
[5] S. Tanabe, K. Hirao, N. Soga, J. Am. Ceram. Soc. 75 (3) (1992) 503.
[6] J.T. Kohli, J.E. Shelby, Phys. Chem. Glasses 32 (2) (1991) 67.
[7] J.T. Kohli, J.E. Shelby, J. Am. Ceram. Soc. 74 (5) (1991) 1031.
[8] J.E. Shelby, S.M. Milton, C.E. Lord, M.R. Tuzzolo, Phys. Chem. Glasses 33 (3) (1992) 93.
[9] M.J. Hyatt, D.E. Day, J. Am. Ceram. Soc. 70 (10) (1987) C283.
[10] J.T. Kohli, J.E. Shelby, Phys. Chem. Glasses 32 (3) (1991) 109.
[11] G.R. Choppin, J. Less-Common Met. 93 (1983) 323.

[12] J.W. Ward, J. Less-Common Met. 93 (1983) 279.
[13] F. David, J. Less-Common Met. 121 (1986) 27.
[14] L.R. Morss, in: C.G. Sombret (Ed.), Mat. Res. Soc. Symp. Proc., 1992, p. 275.
[15] L.R. Morss, C.W. Williams, in: C.G. Sombret (Ed.), Mat. Res. Soc. Symp. Proc., 1992, p. 283.
[16] D. Boust, Thèse de Doctorat – Université de Caen, 1986, 250 p.
[17] K.B. Krauskopf, Chem. Geol. 55 (1986) 323.
[18] J.C. Dran, G. Della Mea, A. Paccagnella, J.C. Petit, M.T. Menager, Radiochim. Acta 44–45 (1988) 299.
[19] E.R. Vance, B.D. Begg, R.A. Day, C.J. Ball, Mat. Res. Soc. Symp. Proc., vol. 353, 1995, p. 767.
[20] B.D. Begg, E.R. Vance, G.R. Lumpkin, In Sci. Basis for Nuclear Waste Management XXI, Mat. Res. Soc. Symp. Proc., vol. 506, 1998, p. 79.
[21] J.T. Kohli, J.E. Shelby, J.S. Frye, Phys. Chem. Glasses 33 (3) (1992).
[22] J.E. Shelby, J.T. Kohli, J. Am. Ceram. Soc. 73 (1) (1990) 39.
[23] M. Ohashi, K. Nakamura, K. Hirao, S. Kanzaki, J. Am. Ceram. Soc. 78 (1) (1995) 71.
[24] R. Ramesh, J. Eur. Ceram. Soc. 17 (1997) 1933.
[25] A. Makishima, M. Kobayashi, T. Shimohira, Commun. Am. Ceramic Soc. C 210 (1982).
[26] S. Sen, J. Non Cryst. Solids 261 (2000) 226.
[27] S. Gavarini, thesis, University of Orleans, France, 2002.
[28] S. Gavarini, P. Trocellier, F. Carrot, G. Matzen, J. Non Cryst. Solids, submitted for publication.
[29] C.H. Baes, R.E. Mesmer, The Hydrolisis of Cations, Wiley, NY, 1976.
[30] R.K. Iler, The Chemistry of Silica, Wiley, New York.
[31] E. Vernaz, T. Advocat, J.L. Dussossoy, Ceramic Trans. 9 (1990) 175.
[32] T.H. Elmer, M.E. Nordberg, J. Am. Ceram. Soc. 41 (12) (1958).
[33] O. Gunnarson, K. Schönhammer, Phys. Rev. B 28 (1983) 4315.
[34] A. Kotani, H. Ogasawara, J. Electron Spectrosc. Relat. Phenom 60 (1992) 257.
[35] M. Romeo, K. Bak, J. El Fallah, F. Le Normand, L. Hilaire, Surf. Interf. Anal. 20 (1993) 508.
[36] T. Nakano, A. Kotani, J.C. Parlebas, J. Phys. Soc. Jpn. 5 (1987) 2201.
[37] N. Thromat, M. Gautier-Soyer, G. Bordier, Surf. Sci. 345 (1996) 290.
[38] S. Gavarini, P. Trocellier, G. Matzen, Y. Vaills, F. Carrot, L. Bois, Nucl. Instrum. and Meth. B 181 (2001) 413.
[39] E. Vernaz, J.L. Dussossoy, Appl. Chem. (Suppl. 1) (1992) 13.
[40] E. Vernaz, S. Gin, C. Jégou, I. Ribet, J. Nucl. Mater. 298 (2001) 27.
[41] E. Vernaz, T. Advocat, J.L. Dussossoy, Ceramic Trans. 9 (2001) 175.
[42] T. Advocat, J.L. Crovisier, E. Vernaz, C.R. Acad. Sci. Paris, Serie II 1991, p. 407.
[43] S. Gin, J.P. Mestre, J. Nucl. Mater. 295 (2001) 83.
[44] W.L. Bourcier, Mat. Res. Soc. Symp. Proc., vol. 212, 1991, p. 3.
[45] S. Guilbert, M.J. Guittet, N. Barré, P. Trocellier, M. Gautier-Soyer, Z. Andriambololona, Radiochim. Acta 90 (2002) 75.